

# DIRECT X-RAY IMAGING FOR THE NEW PINHOLE DIAGNOSTICS AT BESSY II

M. Marongiu\*, V. Dürr, C. Kalus, G. Rehm, M. Ries, A. Schällicke, HZB, Berlin, Germany

## Abstract

In order to improve our transverse diagnostic tools, two new pinhole beamlines will be designed. The pinhole arrays will be in air for easier maintenance: this will result in a significant loss of X-Ray photons when passing through the vacuum window. To overcome this issue, the option to directly illuminate a CCD/CMOS camera with X-Ray radiation without prior conversion into visible light is under study. Tests in the existing beamline both with a conventional CMOS camera and with a dedicated X-Ray camera are foreseen. This report describes our findings regarding the current status regarding the use of X-Ray cameras as a "high flux" diagnostic tool, as well as our preliminary experimental results.

## MOTIVATION

The present BESSY II electron-storage ring of Helmholtz-Zentrum Berlin (HZB) is operated at an electron energy of 1.7 GeV with an RF cavity frequency of 500 MHz [1]. The typical beam current is 300 mA in top-up operation; in Table 1 the more relevant parameters are shown.

Table 1: Main Parameters of BESSY II in Standard Mode Operation

TopUp	Value
Beam Energy (GeV)	1.7
Rel. Energy Spread (%)	$7 \times 10^{-4}$
Beam Current (mA)	300
Beam emittance (nm)	5
Coupling (%)	2
RMS Bunch-length (ps)	20
Bending Magnet Field (T)	1.3
Critical Energy (keV)	2.5
Lin. Pow. Density (Wmrad <sup>-1</sup> )	8.1
Circumference (m)	240

Pinhole camera are used as main X-Ray transverse diagnostic at BESSY [2]; two new beamlines will be installed to indirectly measure both emittance and momentum spread. This possibility is not currently available at the current beamline locations.

Furthermore, in order to allow easier and faster maintenance, the new beamlines will be realized in air, rather than in vacuum; this, however, causes a loss of radiation at the vacuum window that needs to be studied and addressed. One possibility is to directly image the X-Ray radiation, rather

\* marco.marongiu@helmholtz-berlin.de

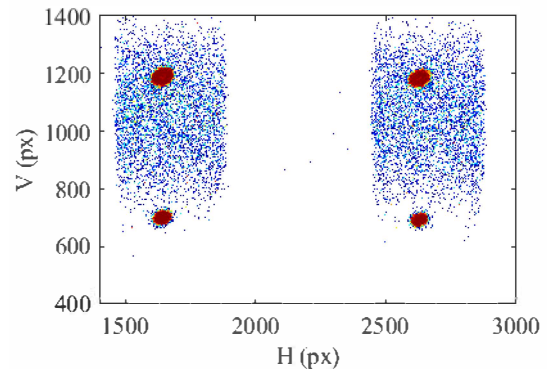


Figure 1: After 3 weeks of operation, an image has been captured by the CMOS camera: the amount of trapped electrons is dominant with respect to the incoming photons. Four beam spots from the pinhole array are visible, and also the radiation fan in the background. The white strip in the middle is due to the cooling grid of the pinhole target [3] (2 mm thick CuBe).

than previously converted it into visible light with a scintillator screen as it is usually done in synchrotron light sources. Some test using conventional visible light camera to directly image the X-Ray are ongoing: in Fig. 1, an example is shown.

## PINHOLE LOCATIONS

In order to be able to measure emittance and momentum spread, a direct measurement of the transverse beam size in two location with significantly different Twiss parameters is needed. A proper evaluation of the optimal locations requires to estimate the propagation of uncertainties of the indirect measure (momentum spread and emittance) as a function of the Twiss parameters and of the directly measured beam sizes. It can be easily proved that the relative uncertainty of the momentum spread, assuming equal relative uncertainties of the beam sizes and negligible uncertainties of the Twiss parameters, is as follow:

$$\frac{U_{\Delta E}}{\Delta E} \propto \frac{\sqrt{1+x^2}}{1-x} \frac{U_{\sigma}}{\sigma}, \quad (1)$$

with  $x = \frac{\sigma_2^2 \beta_1}{\sigma_1^2 \beta_2}$ . A similar relation can be find for the emittance; in this case there is also a factor 2, and  $x = \frac{\sigma_2^2 D_1^2}{\sigma_1^2 D_2^2}$  where  $D$  is the dispersion.

It is therefore possible to check all the possible combination of available location and sort them with respect to the uncertainties.

One other important aspect to take into account in the beamline design is related to the geometric constraints in the facility (i.e. distance of the pinhole target from the radiation source and overall beamline length) that determines the maximum achievable magnification. This strongly affects the resolution and ultimately the beam size uncertainty measurements, hence the momentum spread and emittance uncertainties too.

Taking all this aspect into consideration, the pinhole locations have been found; the expected beam sizes are 83  $\mu\text{m}$  (horizontal) 32  $\mu\text{m}$  (vertical) for the low dispersion beamline and 88  $\mu\text{m}$  (horizontal) 32  $\mu\text{m}$  (vertical) for the high dispersion beamline. In Table 2 the relevant parameters are shown.

Table 2: Twiss Parameters, Geometric Properties and Expected Spot Size and Uncertainties for the Chosen Beamline Locations: L is the Distance Between Pinhole and Dipole, R is the One Between Detector and Pinhole, While M is R/L.

	Low D	High D
Position (m)	185.07	84.54
L (m)	1.92	2.95
R (m)	7.9	4.16
M	4.1	1.4
$\beta_x$ (m)	0.91	0.79
$\beta_y$ (m)	22.6	22.6
$D_x$ (mm)	3	60
$\sigma_x$ ( $\mu\text{m}$ )	83	88
$\sigma_y$ ( $\mu\text{m}$ )	32	32
$\frac{U_\epsilon}{\epsilon}$		$2\frac{U_\sigma}{\sigma}$
$\frac{U_{\Delta E}}{\Delta E}$		$5.5\frac{U_\sigma}{\sigma}$

## FLUX EVALUATION

Another important factor to evaluate is the amount of radiation that will reach the camera, as well as its wavelengths. It can be estimated using the SPECTRA software [4] (see Fig. 2): it is possible to estimate at which photon energies, there still is significant flux, at which is peaked and, with numerical integration, retrieve the total power reaching the detector. It can be done for the total radiation coming from the bending magnet (blue curve where a 1 mrad aperture is assumed) or the radiation coming out of the pinhole (red curve assuming a 10  $\mu\text{rad}$  pinhole aperture). It is also possible to take into account material other than vacuum that causes attenuation of the flux: here, for instance, a 350  $\mu\text{m}$  diamond vacuum window is taken into account together with a 6 m of air (black curve).

The pinhole causes a significant loss of radiation with the total power that lowers from the initial 8.1 W to 188  $\mu\text{W}$ ; taking into account the vacuum window, the power coming out from the pinhole reduces further to 14  $\mu\text{W}$ . Moreover, the diamond act also as an ‘‘high-pass filter’’ cutting out the

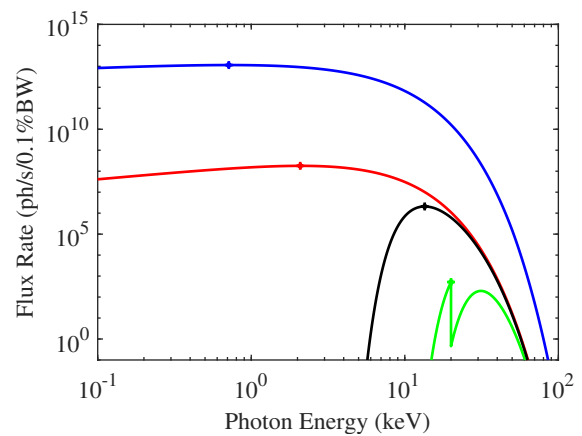


Figure 2: Photon Flux as a function of the photon beam energies. The blue curve represents the total flux coming from the radiation source considering a 1 mrad aperture; the red one represents the flux taking into account the pinhole aperture (about 10  $\mu\text{rad}$ ), the green the flux out of the current beamline (see next section), and the black one takes also into account a 350  $\mu\text{m}$  diamond vacuum window. The asterisks represent the maximum flux available.

low energy part of the radiation (below 6 keV) with the new maxima placed now at an energy of 13 keV.

It is a reduction in power of one order of magnitude with respect to the in-vacuum solution: this may represent an issue, considering that the camera already operates with an exposure time in the order of 100 ms. Taking into account also the magnification changes from 0.3 up to 4.1, hence how the power will be distributed in each pixel, a significant change into the detection mechanism will be needed.

The current beamline uses a scintillator screen to convert the X-Ray radiation into visible light, that is emitted in a  $4\pi$  angle and then partially collected by the optical system and detected by a visible light camera. An alternative to this inefficient way could be instead to image directly the X-Ray with a camera.

## DIRECT X-RAY IMAGING

When the radiation interacts with the sensor of the camera, a certain amount of electron-hole pairs are generated: it can be estimated as the ratio of the photon energy and 3.66 eV (silicon based sensor). The main difficulties in the design of such a scheme is the lack of relevant information regarding the sensor in the X-Ray range: much of the data publicly available refers only to the visible and the infrared part of the spectrum.

Furthermore, other useful information such as thickness and composition of the individual layers that compose the sensor are also not published usually: those data may allow the users to estimate the quantum efficiency (QE) of the sensor at a certain photon energy, and, to some extent, its radiation hardness as it was shown in Ref. [5].

To overcome this issue, some tests in the current beamline have been performed placing a conventional visible light

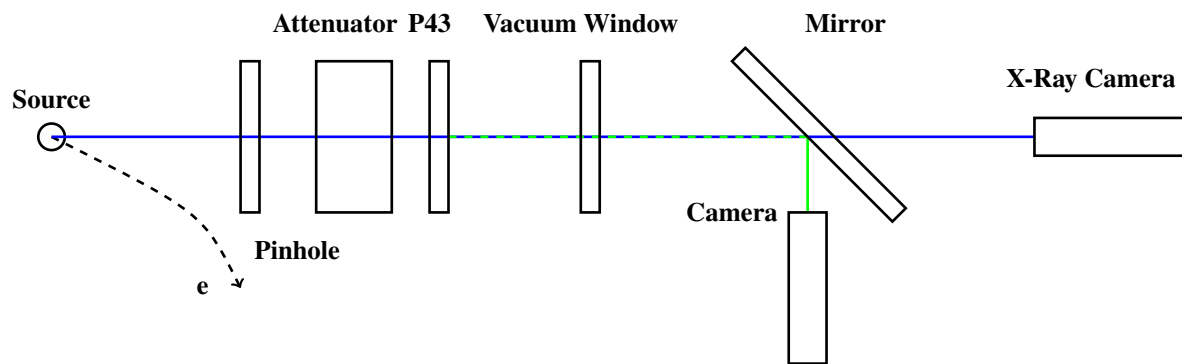


Figure 3: Schematic of the present experimental setup on the existing beamline.

camera behind the scintillator screen: in Fig. 3, a schematic of the setup is shown. Indeed, not all the radiation is absorbed by the scintillator screen and converted into visible light; part of it passes through it and the vacuum window (it consists in an overall 10 mm fused silica and 1 mm aluminum of additional filtering of the spectra), and it has been estimated to be 0.5 nW (see the green curve in Fig. 2).

The tests have been performed at 300 mA, irradiating first a front-illuminated CCD camera sensor [6] and then a backside-illuminated CMOS sensor [7]: sensor of the latter type are also typically used in high-end X-Ray camera [5].

The CCD camera has shown poor performance in term of radiation hardness with damage already visible after about 4 hours of operation; furthermore, significant spillover in neighbor pixels has been observed quickly. After less than 2 weeks, the irradiated part of the sensor was fully saturated even in the absence of the beam.

The CMOS sensor has shown better performances in comparison: there was no spillover and damages start to appear after 2 days around the center of mass of the beam. After 3 weeks of operation, however, also this sensor shows a persistent saturated beam due to trapped electrons, regardless of the eventual incoming radiation. A further one week long experiment at 15 mA causes no visible damage to the sensor instead.

In Fig. 1 it is possible to observe 4 beams spots and also part of the radiation fan: this is due to the fact that the pinhole is made of a 100  $\mu\text{m}$  thick Molybdenum target. The fan looks intermittent because the pinhole is equipped with a cooling grid made of 2 mm thick CuBe [3]: indeed, the large thickness of the grid shields completely the radiation.

The damage of the irradiated area of the sensor is not necessary a big issue in general, since it involves a small amount of pixels with respect of the whole sensor: in the sensor tested, for instance, the damaged area covers a region of interest of less than 20 pixels per side while the whole sensor has around 12 millions of pixels. However, the need to move the sensor very often makes this scheme impractical.

Furthermore, due to the most likely low QE at 20 keV, a clear Gaussian profile is not visible in live-mode, but only after long integration over time. Therefore, additional tests

are required in the future beamline selecting a lower photon energy, hence higher QE.

## OUTLOOK

Two new pinhole beamline will be realized in order to replace the existing one. In the new design, two goals need to be reached: the beamlines need to be in-air to make the maintenance easier and faster and they have to be placed in the proper position in order to measure accurately both emittance and momentum spread.

Evaluating the Twiss parameters evolution along the ring and the different geometric constraints in the tunnel, and applying the propagation of uncertainties, the two beamline locations have been found.

Building the beamlines in-air, however, causes a significant loss of flux in the vacuum window that act like a “high-pass filter”, since the critical energy at BESSY is only 2.5 keV.

A possible solution currently under study is to replace the detection mechanism based on X-Ray to visible light conversion with a direct X-Ray imaging system.

However, for these energy ranges, it is hard to find in literature or in the datasheet the relevant information like quantum efficiency as well as information regarding the radiation hardness.

Therefore, experimental tests with several camera sensor are currently ongoing. Preliminary results indicates that front-illuminated CCD sensors are not well-suited for this operational mode, while backside-illuminated CMOS sensors looks more promising.

However, more experiments need to be done to better characterize the sensor at these energy ranges and radiation fluxes both in term of quantum efficiency and in term radiation hardness.

## ACKNOWLEDGMENT

The authors want to thank P. Ahmels and T. Atkinson for the help in the design and the installation of the experimental setup.

## REFERENCES

- [1] P. Goslawski *et al.*, “BESSY III - status and overview”, in *Proc. IPAC’23*, Venice, Italy, pp. 457–460, 2023.  
doi: 10.18429/JACoW-IPAC2023-MOPA174
- [2] K. Holldack, J. Feikes, and W. Peatman, “Source size and emittance monitoring on BESSY II”, *Nucl. Instrum. Methods Phys. Res. A*, vol. 467, pp. 235–238, 2001.
- [3] K. Holldack, private communication, 2025.
- [4] T. Tanaka, “Major upgrade of the synchrotron radiation calculation code SPECTRA”, *J. Synchrotron Radiat.*, vol. 28, no. 4, pp. 1267–1272, 2021.
- [5] K. Desjardins *et al.*, “Backside-illuminated scientific cmos detector for soft x-ray resonant scattering and ptychography”, *J. Synchrotron Radiat.*, vol. 27, no. 6, pp. 1577–1589, 2020.
- [6] *Prosilica GT 1920 Data Sheet*, Allied Vision Technologies GmbH, 2025. [https://cdn.alliedvision.com/fileadmin/pdf/de/Prosilica\\_GT\\_1920\\_DataSheet\\_de.pdf](https://cdn.alliedvision.com/fileadmin/pdf/de/Prosilica_GT_1920_DataSheet_de.pdf)
- [7] *Raspberry Pi Camera Module 3*, Raspberry Pi Ltd, 2025. <https://datasheets.raspberrypi.com/camera/camera-module-3-product-brief.pdf>